RESEARCH Open Access



Therapeutic effects of adipose tissue-derived mesenchymal stem cells on ER stress in a murine model of metabolic dysfunction-associated steatohepatitis: an in vivo and in vitro study

Norihiko Ogawa¹, Akihiro Seki^{1*}, Alessandro Nasti², Ho Yagi², Masatoshi Yamato^{1,3}, Hiiro Inui¹, Hiroki Nomura¹, Takuya Komura^{1,4}, Hidetoshi Nakagawa¹, Kouki Nio¹, Hajime Takatori¹, Tetsuro Shimakami¹, Masao Honda¹, Shuichi Kaneko², Yoshio Sakai^{1,5} and Taro Yamashita¹

Abstract

Background Metabolic dysfunction-associated fatty liver disease (MAFLD) is an increasing concern due to lifestyle changes, with metabolic dysfunction-associated steatohepatitis (MASH) leading to progressive liver damage, cirrhosis, and increased morbidity. The role of endoplasmic reticulum (ER) stress, particularly the unfolded protein response (UPR) pathway, in MASH progression remains unclear. Adipose tissue-derived stem cells (ADSCs) have shown promise in regenerative therapy; however, their mechanism for alleviating MASH-induced liver damage is not fully understood. In this study, we aimed to investigate the therapeutic mechanism of ADSCs in MASH, focusing on their modulation of ER stress in hepatocytes.

Methods C57BL/6J mice were fed either an atherogenic high-fat diet (AT + HF) or a high-fat diet (HFD-60) to induce MASH and simple steatosis (SS), respectively. Liver tissues were analyzed for gene expression, protein levels, and apoptotic markers using DNA microarray, quantitative PCR, western blotting, histological staining, and caspase activity assays. ADSCs were harvested, cultured, and treated to assess their effects on ER stress. In vitro experiments investigated palmitic acid-induced ER stress in hepatocytes and the effects of ADSCs on hepatic stellate cells and inflammatory markers.

Results The PERK arm of the UPR pathway was significantly upregulated in MASH liver tissues compared to SS tissues, correlating with increased apoptosis. ADSC administration reduced PERK activation, decreased apoptotic marker expression, and ameliorated hepatic fibrosis. However, ADSCs did not directly attenuate palmitic acid-induced ER stress in hepatocytes in vitro. Instead, they modulated the hepatic microenvironment by reducing hepatic stellate cell activation and IL-17-associated inflammation, indirectly mitigating ER stress and hepatocyte apoptosis.

*Correspondence: Akihiro Seki Seki0510@gmail.com

Full list of author information is available at the end of the article



© The Author(s) 2025. **Open Access** This article is licensed under a Creative Commons Attribution-NonCommercial-NoDerivatives 4.0 International License, which permits any non-commercial use, sharing, distribution and reproduction in any medium or format, as long as you give appropriate credit to the original author(s) and the source, provide a link to the Creative Commons licence, and indicate if you modified the licensed material. You do not have permission under this licence to share adapted material derived from this article or parts of it. The images or other third party material in this article are included in the article's Creative Commons licence, unless indicated otherwise in a credit line to the material. If material is not included in the article's Creative Commons licence and your intended use is not permitted by statutory regulation or exceeds the permitted use, you will need to obtain permission directly from the copyright holder. To view a copy of this licence, visit http://creativecommons.org/licenses/by-nc-nd/4.0/.

Conclusions ADSCs alleviate MASH progression by modulating ER stress via immunomodulation rather than through directly rescuing hepatocytes. These findings highlight the potential of ADSCs as an immunomodulatory therapeutic strategy for MASH and support further investigation into their clinical application.

Keywords Metabolic Dysfunction-Associated steatohepatitis, Endoplasmic reticulum stress, Unfolded protein response, Adipose tissue-derived stem cells, Mesenchymal stem cells

Background

Metabolic dysfunction-associated fatty liver disease (MAFLD) is an increasingly prevalent chronic liver condition associated with lifestyle changes [1]. MAFLD encompasses a spectrum ranging from simple steatosis (SS), characterized by lipid accumulation in hepatocytes without associated inflammation, to metabolic dysfunction-associated steatohepatitis (MASH), a more advanced stage marked by hepatocellular injury, inflammation, and fibrosis, often progressing to cirrhosis [2]. Clinically, cirrhosis in patients with MASH is associated with significantly poorer outcomes compared to other forms of chronic liver disease. A major challenge in developing effective treatments for MASH-related cirrhosis is the limited understanding of its underlying mechanisms. Hepatocellular damage, leading to lipid accumulation, is considered the "second hit" in the progression from SS to MASH. This process is driven by multiple pathological factors, including intestinal-derived lipopolysaccharide (LPS), which induces inflammation-induced hepatocyte injury, and oxidative and endoplasmic reticulum (ER) stress [3]. The ER plays a central role in protein folding, lipid and carbohydrate metabolism, and the maintenance of cellular homeostasis [4]. Accumulation of misfolded or denatured proteins in the ER induces ER stress and activates the unfolded protein response (UPR), a protective signaling network designed to restore homeostasis by reducing the protein load. If ER stress persists or becomes excessive, the UPR shifts from an adaptive to a pro-apoptotic response, ultimately leading to cell death [5]. Recent evidence suggests that ER stress is a key contributor to MASH progression [6], potentially acting downstream of LPS signaling and oxidative stress in the diseased liver. Nonetheless, the precise mechanisms by which ER stress contributes to MASH progression remain unclear.

With advances in stem cell research, the application of stem cells in regenerative therapies for organ repair, including chronic liver disease, has garnered significant attention [7]. Stem cells are classified into three main types: embryonic stem cells, induced pluripotent stem cells, and somatic stem cells. Among the latter, mesenchymal stem cells (MSCs), which can be isolated from autologous sources such as adipose tissue, bone marrow, and umbilical cord, are particularly promising due to their ease of collection and minimal ethical or technical concerns. In addition, MSCs are well recognized for their

immunomodulatory properties, making them an attractive option for regenerative treatment strategies. We previously reported that the therapeutic effects of adipose tissue-derived stem cells (ADSCs), a type of MSC, are mediated through interactions with intrahepatic inflammatory cells in MASH [8, 9]. However, the specific biological responses of hepatocytes and non-parenchymal cells to ADSC treatment in MASH remain poorly understood.

In this study, we aimed to investigate the therapeutic mechanism of ADSCs in MASH by focusing on their modulation of ER stress in hepatocytes. Therefore, we employed a murine MASH model and used immortalized murine hepatocyte cell lines.

Methods

Mouse experiments

This study was conducted in accordance with the ARRIVE guidelines for reporting animal research. All animal experiments were conducted in accordance with the experimental protocol approved by the Kanazawa University Animal Experiment Committee (approval no. AP21-019) and complied with Kanazawa University Animal Experiment Regulations at the Institute for Experimental Animals of Kanazawa University. Female C57BL/6J mice (8 weeks old) were purchased from Jackson Laboratory Japan and fed either an atherogenic high-fat diet (AT+HF) or a high-fat diet (HFD-60) to induce MASH and SS models, as described previously [8, 9]. To compare liver tissue characteristics between MASH and SS mice, tissues were harvested at 3, 6, and 12 weeks after diet initiation for subsequent analyses or stored under appropriate conditions for future use. The number of mice was five per diet group at each time point, representing the minimum number required for statistical analysis. Each group was housed in a separate cage per diet. At eight and ten weeks after initiation of AT + HF feeding, 2×10^5 ADSCs were injected into the splenic subcapsule to assess the treatment effect. At twelve weeks after the start of feeding, liver tissues were harvested for subsequent analysis. Mice were grouped randomly, although no special method of randomization was used. To minimize potential confounders, the order of treatments and measurements, as well as positions of animals and cages were randomized. At the time of surgery, medetomidine (0.3 mg/kg), midazolam (4 mg/kg), and butorphanol (5 mg/kg) were administered

intraperitoneally as an esthesia. CO_2 gas was used for euthanasia.

Hepatocyte isolation

Hepatocytes were isolated from liver tissue as previously described [8]. Briefly, liver tissue was enzymatically digested at 37 °C for 30 min using 0.25% collagenase type I (Wako, Osaka, Japan). Hepatocytes were isolated using 40% Percoll° PLUS (GE Healthcare, Chicago, IL, USA) via centrifugation at 2000 rpm for 20 min at room temperature.

Acquisition of adipose tissue-derived mesenchymal stem cells

ADSCs were isolated and cultured as previously described [10]. Briefly, inguinal subcutaneous adipose tissue was harvested from 10- to 12-week-old male C57BL/6J mice. Tissue was enzymatically digested with 0.15% type I collagenase (Worthington Biochemical Corporation, Lakewood, NJ, USA), followed by centrifugation at 620×g to isolate the stromal vascular fraction. Collected cells were then cultured and expanded in Dulbecco's Modified Eagle Medium/Nutrient Mixture F-12 (DMEM/F12) supplemented with 20% heat-inactivated fetal bovine serum (FBS) and 1% antibiotic—antimycotic solution (Life Technologies, Bedford, MA, USA). Cells at passages 5 to 6 were used for subsequent experiments.

Histological and immunohistochemical staining

Liver tissue samples were fixed in IHC Zinc Fixative® (BD Pharmingen, San Jose, CA, USA) and embedded in paraffin. Sections of 2 µm thickness were prepared for hematoxylin and eosin (HE), Azan, and immunohistochemical staining. For immunohistochemistry, 7 µm cryosections were prepared from frozen liver tissues embedded in OCT compound (Sakura Finetek, Tokyo, Japan). Endogenous peroxidase activity was blocked using Peroxidase Blocking Reagent (Agilent Technologies, Santa Clara, CA, USA), and non-specific protein binding was blocked using Protein Block (Agilent). Sections were incubated overnight at 4°C with primary antibodies listed in the Table S1A, followed by a 30-min incubation at room temperature with Histofine[®] Simple Stain[™] Mouse MAX PO, Rat, or Rabbit (Nichirei Bioscience, Tokyo, Japan). Color development was performed using the Histofine DAB Substrate Kit (Nichirei Bioscience), and sections were counterstained with hematoxylin (Nichirei Bioscience).

Cell lines

The mouse hepatocyte cell line H2.35 and mouse Kupffer cell line KUP5 were obtained from DS Pharma Biomedical (Osaka, Japan) and RIKEN BRC (RCB4627; Ibaraki, Japan), respectively [11]. H2.35 cells were maintained in low-glucose D-MEM medium (Wako) supplemented

with 4% FBS (Sigma-Aldrich) and 200 nM dexamethasone (Sigma-Aldrich). KUP5 cells were cultured in high-glucose D-MEM (Wako) containing 10% FBS (Sigma-Aldrich), 10 $\mu g/mL$ bovine insulin, and 250 μM monothioglycerol. The IMS/N murine immortalized hepatic stellate cell line, a kind gift from Dr. Miura [12], was cultured in DMEM (Wako) containing 10% FBS (Sigma-Aldrich), antibiotic-antimycotics (Gibco BRL/Life Technologies), and GlutaMAX (Gibco BRL/Life Technologies). Recombinant IL-17 A (PeproTech, Cranbury, NJ, USA) was added to IMS/N cultures at a final concentration of 100 ng/mL for activation as needed.

In vitro palmitic acid treatment

H2.35 cells were seeded in 6-well plates, with 1×10^5 or 3×10^5 cells per well. Palmitic acid (PA; Sigma-Aldrich), dissolved in 50% ethanol, was added at concentrations ranging from 0.1 mM to 0.4 mM to induce ER stress via lipotoxicity.

Gene expression analysis

Total RNA was extracted from Liver tissue, isolated hepatocytes, H2.35, or IMS/N using the ISOSPIN Cell & Tissue RNA Kit (Nippon Gene, Tokyo, Japan), following the manufacturer's protocol. As for the DNA microarray analysis, RNA obtained from hepatocytes or IMS/N was purified, amplified and labeled with Cy3 with the Quick Amp Labeling Kit (Agilent Technologies, Santa Clara, CA, USA), then complementary RNA was hybridized to the Whole Mouse Genome 4×44 K Array (Agilent Technologies), the Agilent G2505B Microarray Scanner used for the reading. BRB ArrayTools (https://brb.nci.nih.g ov/BRB-ArrayTools/) was used for the gene expression analysis. Filters were set to exclude spots with intensities below 1; quantile normalization was applied. Multiple probes recognizing were reduced to one per gene symbol by selecting the maximally expressed probe. Furthermore, a list of MetaCore pathway maps (MetaCore from Clarivate Analytics, Philadelphia, PA, USA) was obtained following the enrichment analysis of differentially expressing genes identified in the preliminary class comparisons. Microarray data comparing the gene expression of MASH hepatocytes and SS hepatocytes, shown in Fig. 1 were deposited in the NCBI Gene Expression Omnibus database as GSE ID: GSE296715. Microarray data comparing the gene expression of IMS/N, IMS/M activated with IL-17 or palmitic acid, and co-cultured with ADSCs in each condition, were deposited in the NCBI Gene Expression Omnibus database as GSE IDs: GSE296717, GSE296718. As for the qRT-PCR, by using RNAs from liver tissue or H2.35, reverse transcription quantitative PCR was performed using the QuantStudio 12 K Flex Real-Time PCR system (Applied Biosystems, Foster City, CA, USA) with qPCR MasterMix Plus

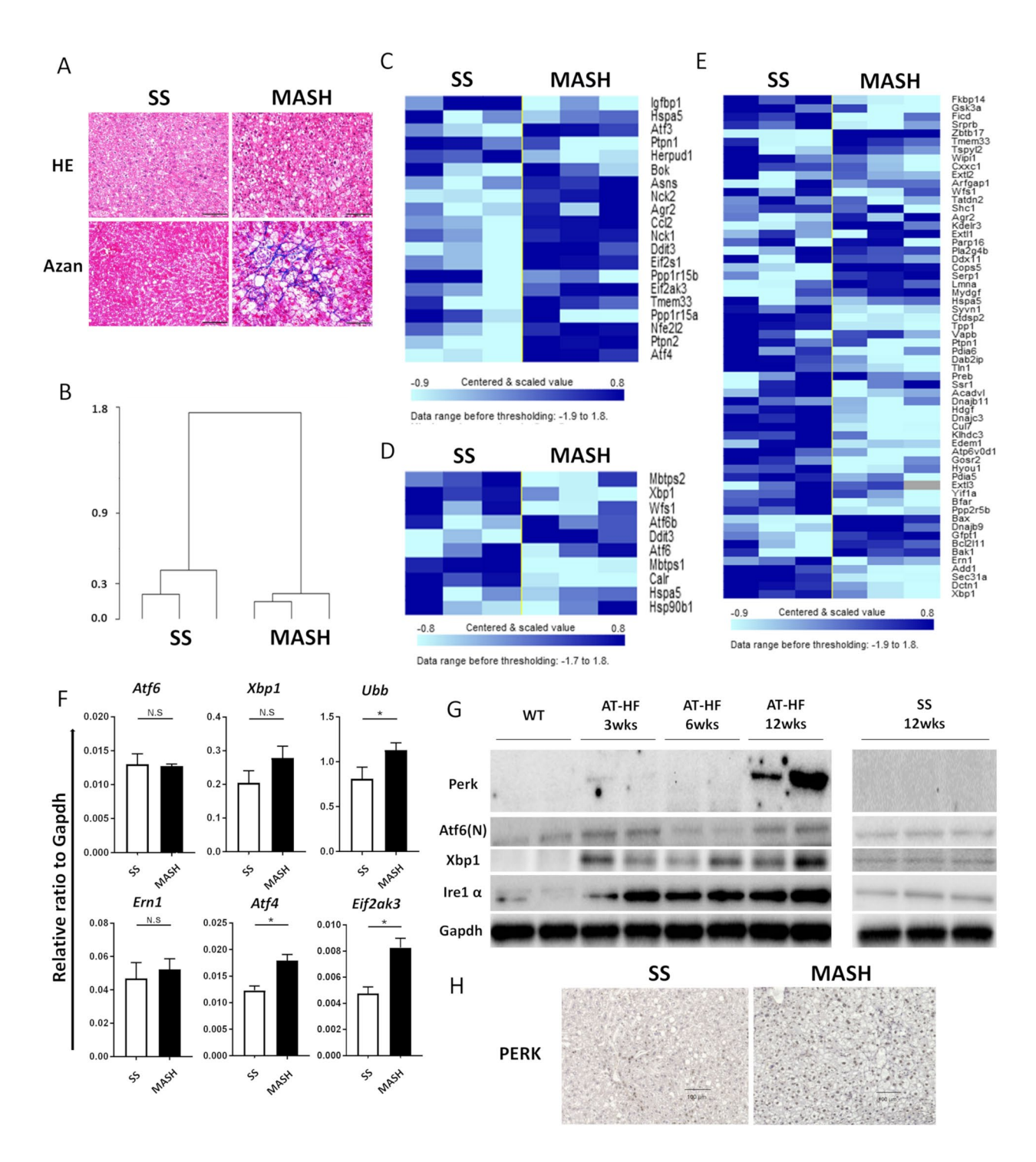


Fig. 1 Comparison of the characteristics of MASH and SS mice. For 12 weeks, mice from the MASH group were fed an atherogenic high-fat diet (AT + HF) while those from the simple steatosis (SS) group received a high-fat diet (HFD-60). For each timepoint, each group consisted of five mice. (**A**) Representative histological images of liver tissues stained with hematoxylin and eosin (HE) and Azan. Scale bars: 100 μm. (**B-F**) Gene expression analysis was performed by DNA microarray using three RNA samples randomly selected from isolated hepatocytes from liver tissue. (**B**) Hierarchical clustering analysis showing gene expression of hepatocytes. Heatmap of gene expression related to the PERK pathway (**C**), the Atf6 pathway (**D**), and the Ire1 pathway (**E**). (**F**) Quantitative real-time PCR (qRT-PCR) validation of UPR-related genes. (**G**) Western blot analysis of UPR-related proteins in liver tissues Full-length blots/gels are presented in Figure S4. (**H**) Immunohistochemical staining of liver tissues with anti-PERK antibody. Scale bars: 100 μm. Data are presented as mean ± SEM (*n* = 5 for each group). **P* < 0.05 indicates statistical significance between MASH and SS groups

(Eurogentec, Seraing, Belgium) and TaqMan Gene Expression Assay probes described in the Table S1B (Thermo Fisher scientific, Waltham, MA, USA).

Western blotting

Proteins were extracted from hepatocyte cell lines and liver tissues using RIPA lysis buffer (Upstate Biotechnology, Boston, MA, USA) supplemented with PhosSTOP (Roche, Basel, Switzerland). Protein concentrations were determined using the Lowry method. After normalization, 20 µg of protein per 10 µL sample was loaded onto a 5-20% SuperSep Ace polyacrylamide gel (13-well format; Wako) for sodium dodecyl sulfate-polyacrylamide gel electrophoresis (SDS-PAGE) separation. Proteins were transferred onto Immobilon°-P polyvinylidene fluoride (PVDF) membranes (Merck, Darmstadt, Germany), blocked with 5% skim milk prepared in TBS-T (25 mM Tris-HCl, pH 7.4; 138 mM NaCl; 2.7 mM KCl; 0.5% Tween 20) at room temperature for 1 h. After washing with TBS-T, membranes were incubated with primary antibodies (dilutions listed in Table S1C), followed by horseradish peroxidase (HRP)-conjugated rabbit antimouse IgG secondary antibody (Cell Signaling Technology, Danvers, MA, USA) diluted 1:1000 and incubated for 1 h at room temperature. Chemiluminescence signals were visualized using Clarity Western ECL Substrate (Bio-Rad Laboratories, Hercules, CA, USA).

Apoptosis assay

- 1) *TUNEL staining*: Liver tissues from MASH model mice were fixed in IHC Zinc Fixative (BD Pharmingen), embedded in paraffin, and stained using the TUNEL Assay Kit-HRP-DAB (Abcam), according to the manufacturer's instructions.
- 2) Caspase assay: Liver tissue Sect. (20 µm per sample) from MASH model mice were homogenized in lysis buffer containing PhosSTOP (Roche) and 10x RIPA Lysis Buffer (Upstate). Resulting supernatants were analyzed for caspase-3/7 activity using the Caspase-Glo 3/7 Assay System and GloMax Multi + Detection System (Promega), according to the manufacturer's protocol.
- 3) Flow cytometry: For in vitro apoptosis assessment, cells were stained with APC- or FITC-conjugated Annexin V (BD Pharmingen) and 7-AAD for 15 min in the dark at room temperature, with gentle shaking. After washing, samples were analyzed using a FACSAccuri cytometer (BD Biosciences, Franklin Lakes, NJ, USA), and data were processed with FlowJo V10 software (Tree Star, Ashland, OR, USA).

Immunofluorescence staining

IMS/N cells were seeded at 0.2×10^5 on BD Falcon CultureSlides (4-chamber, polystyrene, tissue-culture-treated glass slide). After 24 h, 0.5 mM palmitic acid, IL-17, and ADSC-conditioned medium were added under specified conditions. After 48 h, cells were fixed with methanol, blocked with 1% BSA in PBS, and incubated overnight at 4 °C with anti-alpha smooth muscle actin (α -SMA) antibody (primary antibody, ab5694, Abcam) diluted 1:500. After washing, Alexa Fluor * 594-conjugated goat antirabbit IgG H&L (secondary antibody, ab150080 Abcam), diluted 1:500, was added and incubated in a dark place for 30 min. Slides were mounted with VECTARSHIELD Mounting Medium (Vector Laboratories, Newark, CA, USA) and imaged using a fluorescence microscope (BZ-X800; KEYENCE, Japan).

Multiplex cytokine assay

Recombinant IL-17 A (PeproTech) was added to IMS/N cultures at a final concentration of 100 ng/mL, followed by incubation for 24 h. Supernatants were collected and stored at -80 °C. Cytokine concentrations were quantified using the Bio-Plex Pro Mouse Cytokine 23-plex Assay kit (Bio-Rad Laboratories) on the Bio-Plex Suspension Array System (Bio-Rad Laboratories), according to the manufacturer's protocol.

Statistical analysis

Statistical analysis was conducted using PRISM 9 (Graph-Pad Software, San Diego, CA, USA). Unpaired two-tailed Student's t-tests were used for comparing reverse transcription quantitative PCR, immunohistochemistry, and cytokine assay data. P-values < 0.05 were considered statistically significant. Data analysis was performed by Dr. Seki (blinded to group assignment), while experimental allocation and animal testing were conducted by Dr. Ogawa and Dr. Inui (aware of group allocation).

Results

The PERK pathway is upregulated in the livers of MASH model mice

MASH is characterized by hepatic inflammation and fibrosis in the context of MASLD and often coexists with SS. We established MASH and SS mouse models by feeding mice AT + HF and HFD-60 diets, respectively, for 12 weeks, as previously described [9]. Both models demonstrated hepatic lipid accumulation (Fig. 1A, top). However, only MASH mice developed significant inflammatory cell infiltration and progressive hepatic fibrosis, distinguishing the MASH hepatic microenvironment, which consists of hepatocytes, non-parenchymal cells, and infiltrating immune cells, from that of SS (Fig. 1A, bottom).

To investigate molecular differences, hepatocytes were isolated from MASH and SS mice, and gene expression profiles were compared using DNA microarray analysis. Hierarchical clustering of 3,363 genes revealed distinct transcriptional patterns between the two groups. Pathway enrichment analysis identified a marked upregulation of genes associated with the PERK branch of the UPR in hepatocytes from MASH mice, whereas the IRE1 and ATF6 pathways were not similarly activated (Fig. 1C, D, E). ER stress is mediated by three primary transducers-PERK, IRE1, and ATF6-each of which activates specific downstream pathways in response to the accumulation of unfolded proteins [13]. The PERK pathway, in particular, is known to contribute to apoptosis in MASH livers [14]. We validated the transcriptional activation of the PERK pathway by reverse transcription quantitative PCR, confirming elevated expression of Atf4 and Eif2ak3, key effectors of this pathway [15]. In contrast, the expression of genes associated with the ATF6 and IRE1 arms of the UPR, including ATF6, Xbp1, Ubb, and Ern1, remained unchanged in MASH livers (Fig. 1F). Furthermore, PERK expression was significantly increased in the liver tissue of MASH mice after 12 weeks of AT+HF feeding (Fig. 1G). Immunohistochemical staining confirmed that PERK protein and UPR proteins involved in the PERK pathway, such as ATF4, were highly expressed in the liver of MASH model mice than in SS mice (Fig. 1H, S1). These results collectively indicate that hepatocytes in MASH mice experience more severe ER stress than those from SS mice, primarily through selective activation of the PERK pathway.

ADSC administration ameliorates apoptosis and PERK expression in the livers of MASH model mice

Various factors contribute to the development and progression of MASH, with ER stress recently identified as a key pathological component [16]. In our previous study, we confirmed that our cultured ADSCs expressed stem cell surface markers, including CD29, CD44, CD90, and CD105 [17], and we demonstrated that ADSC treatment improved fibrosis and inflammation while enhancing tissue regeneration in MASH model mice [9]. Building on these findings, we assessed whether the therapeutic effects of ADSCs were mediated through modulation of ER stress pathways. ADSCs were administered to MASH model mice, and changes in UPR signaling were evaluated. PERK proteins and gene expression in liver tissues were significantly reduced following ADSC treatment, whereas expression of IRE1 and ATF6 pathway components remained unchanged (Fig. 2A, B). Given that the PERK-ATF4 axis induces apoptosis [18], we examined hepatocyte apoptosis using TUNEL staining. A marked reduction in TUNEL-positive hepatocytes was observed in MASH livers, which was significantly attenuated by ADSCs (Fig. 2C, D). Similarly, the activity of caspase 3/7, a key mediator of apoptosis, was increased in the liver of MASH model mice but significantly decreased after ADSC treatment (Fig. 2E). These results suggest that ADSCs reduce hepatocyte apoptosis by selectively suppressing the PERK pathway during ER stress in the MASH liver.

ADSCs do not directly attenuate ER stress in hepatocytes induced by fatty acids in vitro

Palmitic acid, the most abundant saturated fatty acid in the human body [19], has been reported to induce ER stress and hepatocyte apoptosis in vitro [20]. To investigate whether ADSCs directly mitigate ER stress, we conducted in vitro co-culture experiments using the immortalized mouse hepatocyte cell line H2.35 and PA [21]. First, we confirmed that PA treatment induces ER stress and apoptosis in H2.35 cells. When 0.4 mM PA was added to the culture medium, lipid accumulation was observed in the cytoplasm of H2.35 cells within 24 h (Fig. 3A). Dose-dependent increases in PA concentration led to an increase in PERK protein expression (Fig. 3B) and a reduction in H2.35 cell proliferation (Fig. 3C). To assess whether ADSCs could directly attenuate PAinduced ER stress, H2.35 cells were co-cultured with ADSCs in the presence of 0.4 mM PA (Fig. 3D). Co-culture with ADSCs did not restore lipid accumulation or cell viability of H2.35 (Fig. 3A, E). Furthermore, while PA-treated H2.35 cells showed increased expression of Eif2ak3, a PERK gene, and Atf4, a gene involved in the PERK pathway, UPR-related gene expression remained unchanged in co-culture with ADSCs (Fig. 3F). These results suggest that ADSCs do not directly alleviate fatty acid-induced ER stress or apoptosis in hepatocytes under these in vitro conditions.

ADSC treatment attenuates hepatic stellate cell activation and reduces hepatocyte UPR gene expression

Given that ADSCs did not directly attenuate fatty acidinduced ER stress in hepatocytes in vitro, we next explored whether their effects were mediated through interactions with non-parenchymal cells in the hepatic environment. Specifically, we evaluated the impact of ADSC treatment on hepatic stellate cells and immune cell infiltration in MASH model mouse livers using immunohistochemical staining. The area of α-SMApositive staining, indicative of activated hepatic stellate cells, was markedly increased in MASH livers, but this activation was significantly attenuated following ADSC treatment (Fig. 4A, B). Furthermore, we observed increased infiltration of F4/80-, Gr-1-, CD4-, and CD8apositive immune cells in MASH livers. ADSC treatment selectively reduced the number of Gr-1-positive cells, while the numbers of F4/80-, CD4-, and CD8a-positive

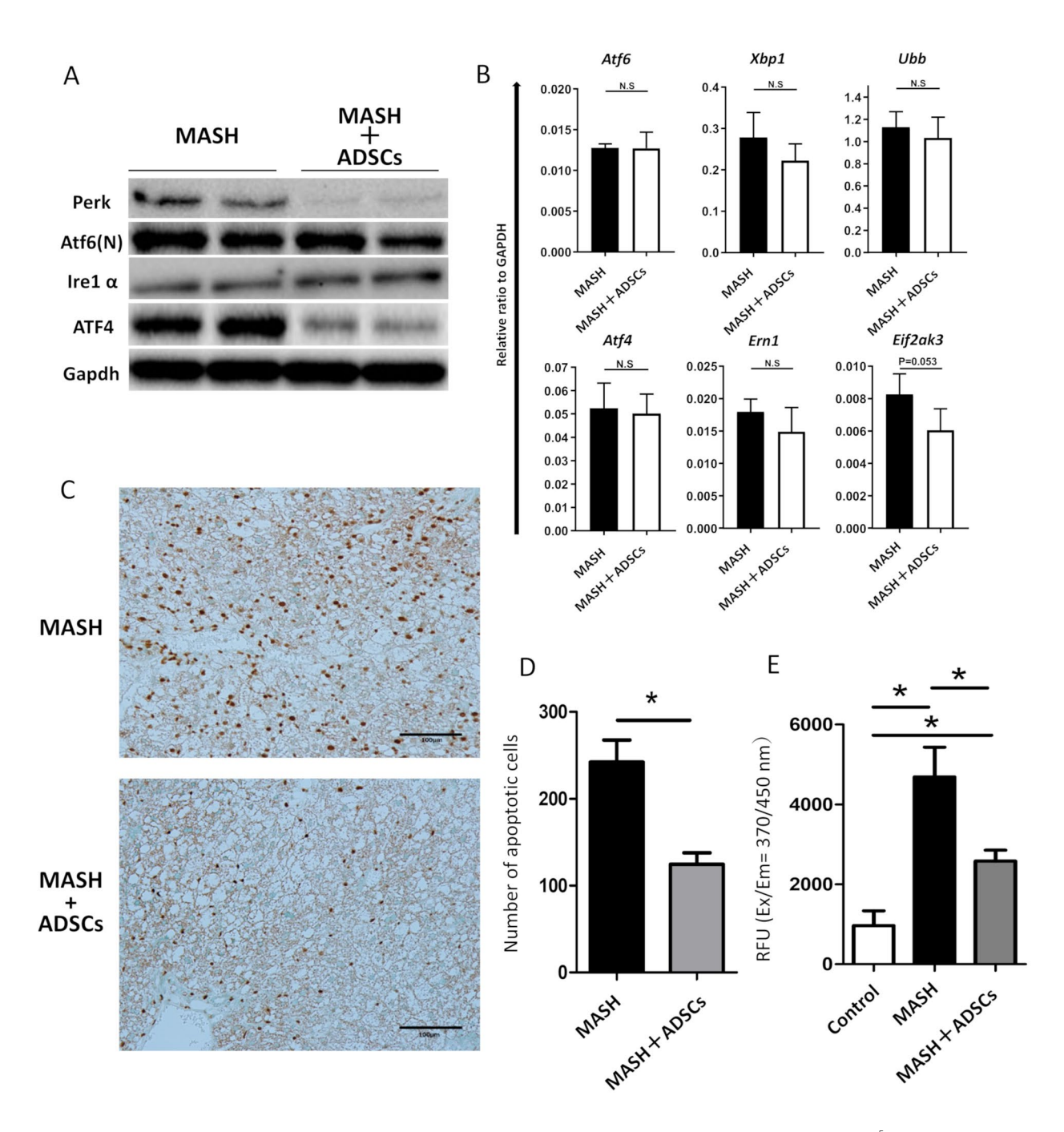


Fig. 2 Therapeutic effect of ADSCs on MASH mice. Eight and ten weeks after the initiation of AT+HF feeding, ADSCs (2×10^5) were injected into the splenic subcapsule. Liver tissues were harvested 12 weeks after the initiation of feeding. Each group consisted of five mice. (**A**) Western blot analysis of UPR-related protein molecules in liver tissues. Full-length blots are presented in Figure S5. (**B**) Quantitative real-time PCR (qRT-PCR) analysis of UPR-related gene expression. Data include mice treated with ADSCs or untreated controls (injected with PBS). (**C**) TUNEL staining of liver tissues to detect apoptotic cells. Magnification: $\times 200$; scale bars: $100 \, \mu m$ (**D**). Quantification of TUNEL-positive cells. (**E**) Caspase 3/7 activity assay. Data are presented as mean \pm SEM (n = 5 for each group). *P < 0.05 indicates statistical significance between groups

inflammatory cells remained unchanged (Fig. S2). α -SMA is a well-established marker of hepatic stellate cells, and these data suggest that ADSCs ameliorate the activation of hepatic stellate cells. Recent studies have shown that hepatic stellate cells can be activated by

IL-17 [22], and we previously reported that IL-17 and its related gene expression are elevated in intrahepatic immune cells (HICs) from MASH mice compared to SS controls [9]. In the current study, IL-17 stimulation increased α -SMA expression in the IMS/N stellate cell

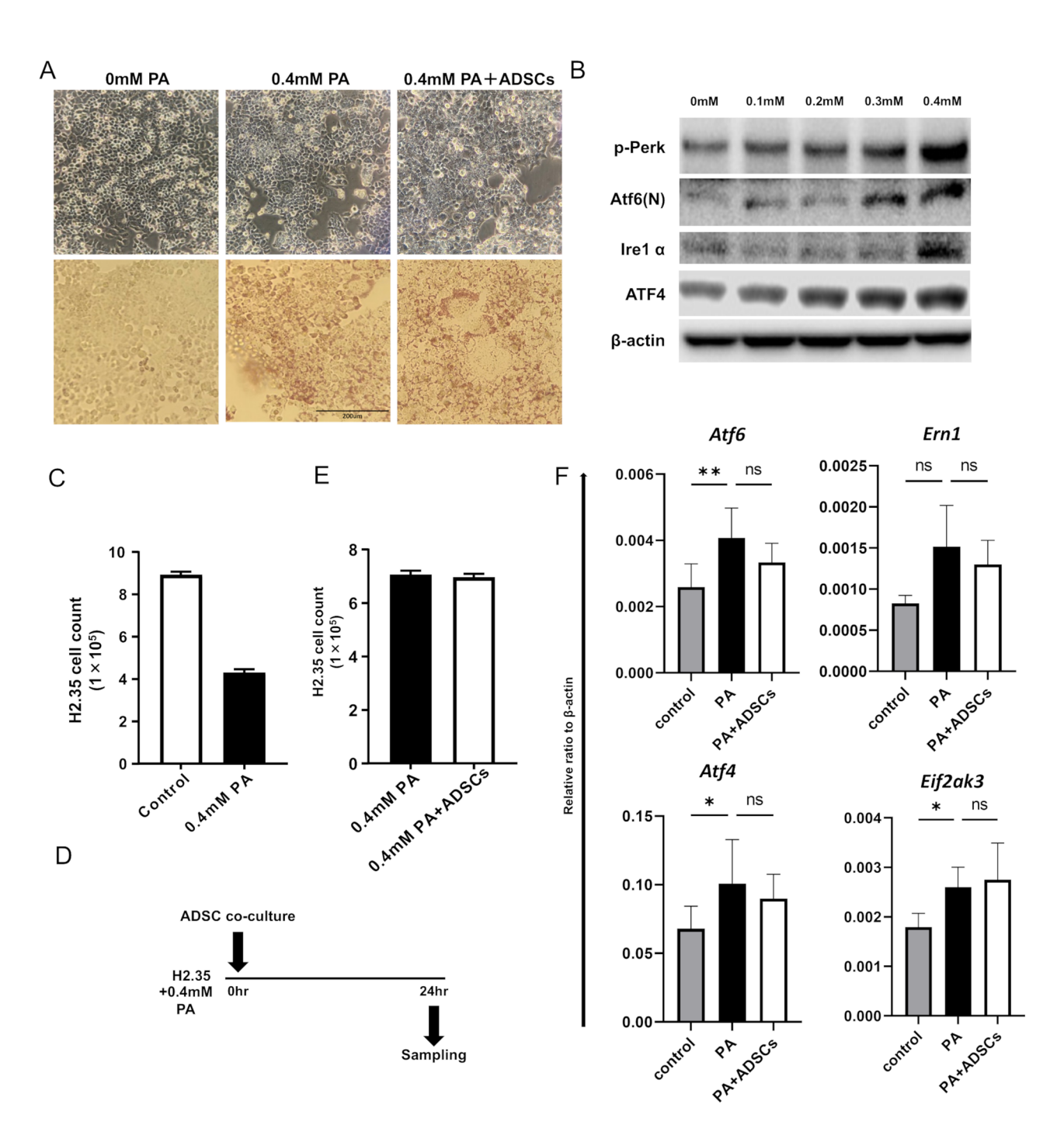


Fig. 3 Steatohepatitis hepatocyte model using H2.35 with palmitate to assess the effects of ADSCs on the ER stress reduction. H2.35 hepatocytes were cultured with 0.4 mm palmitic acid (PA) and co-cultured with ADSCs using culture inserts. (**A**) Evaluation of lipid accumulation by Oil Red O staining (left: control (no PA), middle: PA, right: PA + ADSCs). (**B**) Western blot analysis of UPR-related proteins in the steatohepatitis hepatocyte model. Full-length blots are presented in Figure S6. (**C**) Viable cell count using the trypan blue exclusion method, with counting of H2.35 cells in control and 0.4 mM PA conditions. (**D-F**) ADSC co-culture experiments in 0.4 mM PA-supplemented culture. H2.35 was seeded on 12-well plates at a concentration of 1×10^5 cells/well. (**D**) Schematic diagram of the experiment schedule. (**E**) Viable cell count using the trypan blue dye exclusion method between 0.4 mM PA and 0.4 mM PA + ADSCs conditions (n = 3 for each group). (**F**) Quantitative real-time PCR (qRT-PCR) analysis of UPR-related molecules for H2.35 in ADSC co-cultures under 0.4 mM PA-containing culture media or control, without PA and ADSC. The expression level was assessed compared to that of the β-actin reference gene (at least n = 5 for each group). Data are presented as mean ± SEM. *P < 0.05 indicates statistical significance between groups

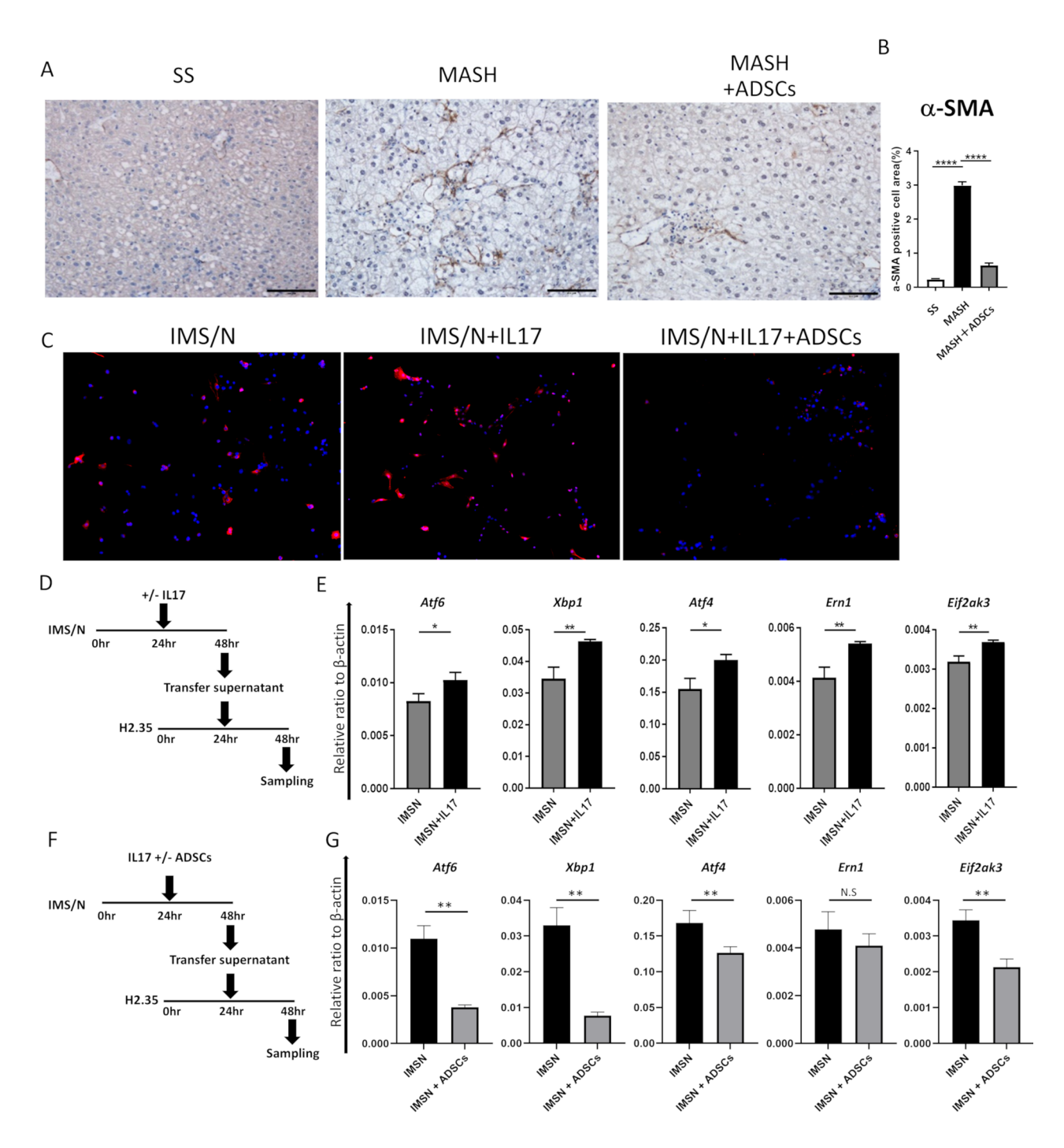


Fig. 4 ADSC treatment attenuates hepatic stellate cell activation and UPR gene expression in MASH mice. (**A, B**) At 8 and 10 weeks after the initiation of AT+HF feeding, ADSCs (2×10^5 cells) were administered into the splenic subcapsule. Liver tissues were harvested two weeks after the last injection. (**A**) Immunohistochemical staining of liver tissues with anti-α-SMA antibody. Each scale bar: 200 μm. (**B**) Quantification of α-SMA-positive cell number or area using ImageJ. Data represent mean ± SEM (n=5). **P<0.01, *****P<0.001. (**C**) Immunofluorescence staining of α-SMA in IMS/N cells cultured with or without PA and co-cultured with or without ADSCs. Magnification: ×200; scale bars: 100 μm. (**D-E**) IMS/N was cultured with an IL-17 supplement for 24 h. H2.35 was seeded in 12-well plates. Twenty-four hours after seeding, the medium was replaced with the IL-17-activated IMS/N supernatant. (**D**) Experimental timeline schedule. (**E**) Quantitative real-time PCR (qRT-PCR) analysis of UPR-related molecules in H2.35 cells cultured with IL-17-activated IMS/N supernatant. The expression level was assessed compared to that of the β-actin reference gene (n=5 for each group). *P<0.05, **P<0.01. (**F**) Experimental timeline schematic for ADSC co-cultured with IL-17 activated IMS/N supernatant. (**G**) qRT-PCR analysis of UPR-related molecules in H2.35 cells co-cultured with ADSCs and IL-17-activated IMS/N supernatant. The expression level was assessed compared to that of the β-actin reference gene. Data represent mean ± SEM (n=5 for each group). *P<0.05, **P<0.05, **

line, confirming activation. However, this activation was markedly suppressed when IMS/N cells were co-cultured with ADSCs, as shown by immunofluorescence assessment (Fig. 4C). To determine whether activated stellate cells contribute to hepatocyte ER stress, we investigated the effect of conditioned media from IL-17-stimulated IMS/N cells on UPR gene expression in H2.35 hepatocytes. Exposure to the supernatant from IL-17-treated IMS/N cells increased UPR gene expression in H2.35 cells (Fig. 4D, E), but not with IL-17 alone or the supernatant from IL-17-treated KUP5 cells, which are immortalized Kupffer cells (Fig. S3A, B). Notably, this effect was diminished when IMS/N cells were co-cultured with ADSCs before collecting the conditioned media (Fig. 4F, G). These results suggest that ADSCs indirectly suppress ER stress in hepatocytes by modulating the activation state of hepatic stellate cells in the MASH liver microenvironment.

PA-stimulated IMS/N supernatant induces apoptosis and enhances UPR in H2.35 cells, with ADSCs mitigating these effects

In addition to the ability of PA to induce ER stress and apoptosis in hepatocytes, we examined whether PA influences hepatic stellate cells in a manner that indirectly promotes ER stress in hepatocytes. H2.35 hepatocytes were cultured with conditioned media from PA alone, untreated IMS/N cells, or IMS/N cells treated with PA. We assessed the impact of these treatments on unfolded UPR gene expression in hepatocytes. Compared to PA or IMS/N supernatant alone, the combination of PA and IMS/N supernatant significantly increased expression of Atf4 and EifAK3, genes in the PERK pathway of the UPR, in H2.35 cells (Fig. 5A). Moreover, H2.35 cells cultured in this combined condition medium exhibited a significant increase in apoptosis, as indicated by annexin V and 7-AAD staining (Fig. 5B). Immunofluorescence analysis confirmed that PA treatment increased IMS/N activation, as evidenced by increased α -SMA levels. However, co-culture with ADSCs attenuated this activation (Fig. 5C). Furthermore, caspase-3 activity, a key indicator of apoptosis in H2.35 hepatocytes, was increased in response to conditioned media from IMS/N cells treated with IL-17 or the combination of IL-17 and PA. Notably, ADSC co-culture suppressed caspase-3 activation under both conditions (Fig. 5D). These results suggest that ADSCs mitigate ER stress and apoptosis in hepatocytes by modulating the activity of hepatic stellate cells.

To further explore the mechanism underlying stellate cell-mediated ER stress, we analyzed gene expression profiles in IMS/N cells activated by IL-17 or PA and compared them to profiles from cells co-cultured with ADSCs. The addition of IL-17 or PA increased the expression of genes involved in interferon (IFN) signaling

in IMS/N, whereas the expression of these gene groups decreased in co-culture with ADSCs. In addition to IFN pathway genes, expression of cytokine genes related to inflammasome signaling was also induced (Tables S2–S5). We then examined cytokine production in the culture supernatants of IMS/N and activated IMS/N cells. Activation with IL-17 or PA increased secretion of proinflammatory cytokines, including IFN- γ , IL-6, TNF- α , MCP-1, Eotaxin, and KC (Fig. 5E). These findings suggest that ER stress and apoptosis in hepatocytes may be induced by a combination of these inflammatory cytokines released from activated stellate cells.

Discussion

This study introduces a novel therapeutic approach for MASH by employing ADSCs to modulate ER stress in hepatocytes. ER stress is a key contributor to MASH progression, interacting with oxidative stress, proinflammatory cytokines, microbiota-derived metabolites, and excessive lipid accumulation to exacerbate liver injury. Activation of the ER stress response, particularly the PERK pathway, leads to caspase-mediated apoptosis in hepatocytes [23, 24]. In our MASH mouse model, we observed elevated hepatocyte apoptosis and caspase-3/7 activity. Importantly, ADSC treatment effectively reduced both apoptosis and caspase activation, suggesting a promising mechanism of action that may attenuate disease progression.

Although ER stress is traditionally associated with lipotoxicity caused by saturated fatty acids such as PA, accumulating evidence highlights internal signals, particularly inflammatory cytokines including IFN-γ [23] and IL-1β [24], as critical drivers of ER stress in various organs. We used PA-treated immortalized hepatocytes (H2.35) to confirm that PA induces UPR activation and apoptosis. However, supernatants from PA-stimulated hepatic stellate cells (IMS/N) enhanced this effect, suggesting that stellate cells play a supportive role in ER stress propagation. These findings support a model in which hepatocyte ER stress is not only a result of direct lipotoxicity but is also amplified by cytokines and paracrine factors secreted by activated stellate cells. This mechanism is consistent with prior reports of stellate cells acting as immune modulators in the liver via secretion of IFN-γ [25], IL-1β, or TNF- α [26], which have been detected in the supernatant of activated immortalized hepatic stellate cells.

ADSCs, which are readily obtained from subcutaneous adipose tissue, are valued for their multipotency, self-renewal capacity, and immunomodulatory properties. These characteristics make them suitable for use in regenerative medicine, including their approved use in Crohn's disease-associated fistulas [27]. MSCs derived from bone marrow have also demonstrated clinical efficacy in treating graft-versus-host disease [28]. In the context of liver

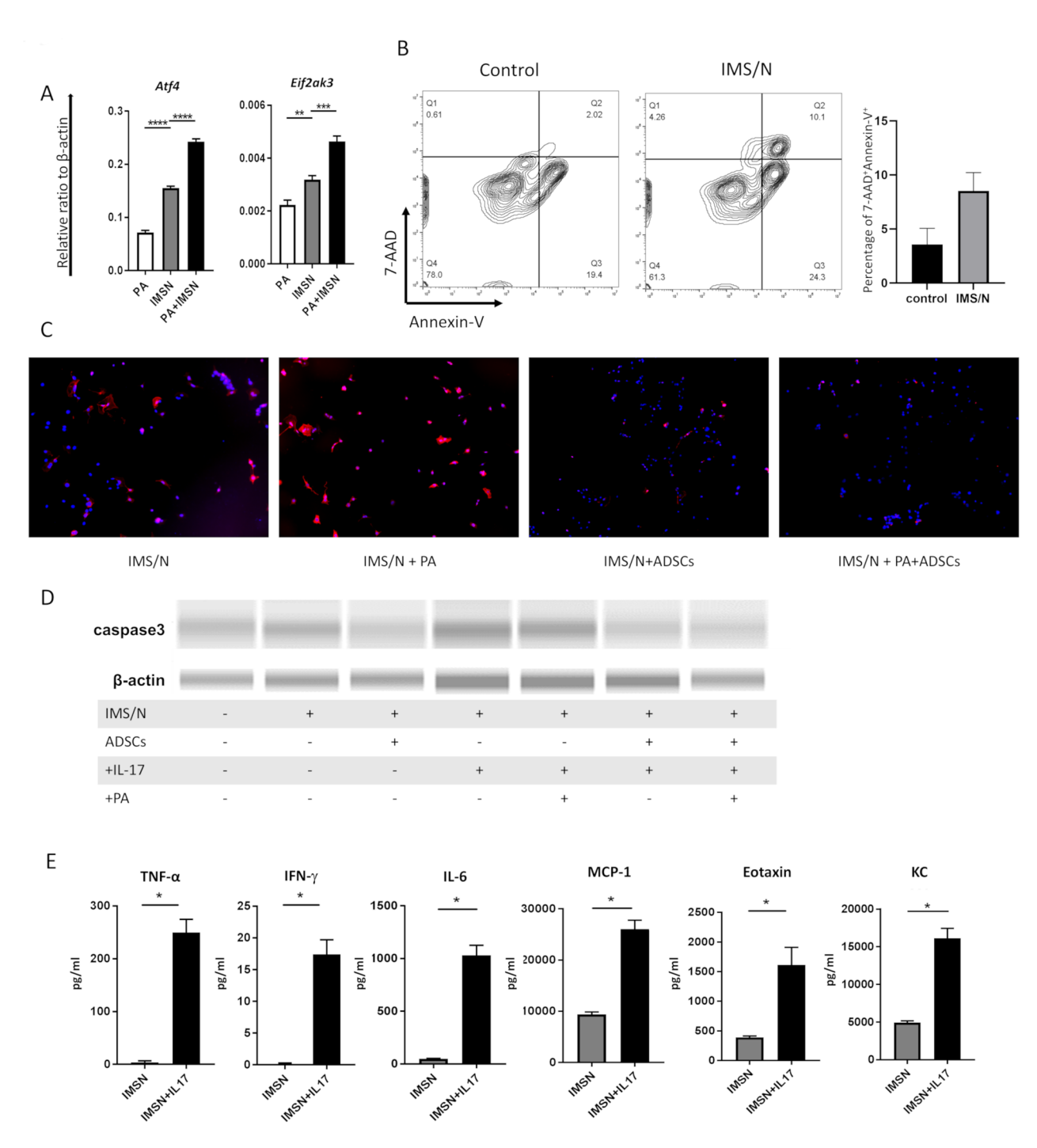


Fig. 5 ADSCs mitigate palmitic acid-activated IMS/N-induced apoptosis and UPR in H2.35 cells in vitro. H2.35 hepatocytes were cultured with supernatants from IMS/N stellate cells pre-treated with 0.4 mM palmitic acid (PA), with or without ADSC co-culture, to evaluate ER stress and apoptosis. (**A**) Gene expression analysis of UPR-related markers in H2.35 cells cultured with PA-activated IMS/N supernatant was performed using qRT-PCR (n=3 per group). **P<0.005, ****P<0.005, *****P<0.005, *****P<0.005, *****P<0.005, *****(D) Immunofluorescence staining of α-SMA in IMS/N cells cultured with or without PA and co-cultured with or without ADSCs. Magnification: ×200; scale bars: 100 μm. (**D**) Western blot analysis of cleaved caspase-3 in H2.35 cells cultured with the supernatant of IMS/N exposed to IL-17 or both IL-17 and PA, with or without ADSC co-culture. Full-length blots are presented in Figure S7. (**E**) Cytokine production by IMS/N cells was measured by multiplex cytokine assay after IL-17 or PA stimulation, with or without ADSC co-culture. Data are expressed as mean ± SEM (n=5 per group), *P<0.05

fibrosis, the presence of ADSCs at least two weeks after administration in MASH cirrhotic liver was confirmed using GFP transgenic mice [8], and ADSCs have been shown to exert beneficial effects through the modulation of hepatic stellate cell function [9]. IL-17, a cytokine known to be increased in MASH-associated cirrhosis, has been identified as a potent activator of hepatic stellate cells [29]. In our study, IL-17 stimulation increased α-SMA expression in IMS/N cells and hepatic stellate cells from MASH model mice. However, ADSC co-culture significantly attenuated this activation, indicating a key immunomodulatory role. These findings support the hypothesis that ADSCs mitigate ER stress in hepatocytes by altering the inflammatory and fibrogenic activity of hepatic stellate cells rather than through direct action on hepatocytes themselves.

While this study provides several important insights into the pathogenesis of MASH and suggests a novel therapeutic mechanism involving ADSCs, it has a few limitations. First, it relied on a murine model, which may not fully replicate human MASH pathology. Second, while we demonstrated a correlation between cytokine signaling and ER stress, direct mechanistic inhibition (e.g., neutralizing antibodies or receptor knockdown) was not performed. Third, only immortalized cell lines were used for in vitro experiments, which may not entirely represent primary hepatocyte or stellate cell behavior. For example, immortalized cells may not share the same cell cycle, gene expression, and metabolic characteristics as primary cells due to several factors including genetic modification. This may result in differences in responses to lipotoxicity and ER stress. Finally, the long-term durability and functional impact of ADSC treatment on fibrosis resolution were not assessed.

The results of the current study offer several key implications for future research and therapeutic development. First, it identifies hepatic stellate cells as key mediators of ER stress in hepatocytes, offering a new cellular target for anti-fibrotic therapies. Second, it suggests that regenerative cell therapies may be more effective when designed to modulate the liver immune niche rather than hepatocytes directly. Future studies should focus on validating these mechanisms in human tissues, as confirmation in clinically relevant samples is critical for translating preclinical insights into therapeutic strategies. Equally important is the thorough evaluation of the long-term effects of ADSC treatment, including sustained therapeutic efficacy over time and comprehensive assessments of safety.

Conclusions

This study demonstrates that ER stress plays a central role in MASH progression and that ADSCs alleviate disease severity by suppressing hepatic stellate cell activation rather than acting directly on hepatocytes. Our findings highlight a novel, indirect mechanism by which ADSCs modulate the hepatic microenvironment to reduce ER stress and hepatocyte apoptosis, mediated through fatty acid- and cytokine-induced stellate cell activity. These results highlight the potential of ADSCs as an immuno-modulatory therapeutic strategy for MASH, particularly in targeting stromal-immune interactions within the liver.

Abbreviations

ADSC Adipose tissue-derived stem cells
AT+HF Atherogenic high-fat diet
DMEM Dulbecco's modified Eagle medium

ER Endoplasmic reticulum FBS Fetal bovine serum

HFD-60 High-fat diet

HIC Hepatic parenchymal cells and intrahepatic inflammatory cells

LPS Lipopolysaccharide

MAFLD Metabolic dysfunction-associated fatty liver disease
MASH Metabolic dysfunction-associated steatohepatitis

MSC Mesenchymal stem cells SS Simple steatosis

UPR Unfolded protein response

Supplementary Information

The online version contains supplementary material available at https://doi.or q/10.1186/s13287-025-04482-4.

Supplementary Material 1

Acknowledgements

We sincerely thank Ms. Maki Wakabayashi for her excellent technical assistance. We would like to thank Editage (www.editage.jp) for English language editing.

Author contributions

NO, AS, MY, HI, TK, YS, TY: conceptualization, methodology, validation; NO, AS: data curation; NO, AS, SI, HY, HI, HN: investigation; NO, AS, AN, HI: formal analysis; AS, YS, TY: funding acquisition, resources; AS, SY, TY: project administration, supervision; NO, AS, AN, HY, HN, KN, HT, TS, MH, SK, YS, TY: writing—original draft. All authors have approved the final manuscript for submission.

Funding

This work was supported by JSPS KAKENHI Grant Numbers 20K17017, 22K15991 and 25K11248.

Data availability

The datasets used during the current study are available from the corresponding author upon reasonable request, and gene expression data analyzed in this research were deposited in the NCBI Gene Expression Omnibus database with GSE IDs: GSE296715, GSE296717, GSE296718.

Declarations

Ethics approval and consent to participate

All animal experiments conducted in this study were approved by the Institutional Animal Care and Use Committee at Kanazawa University under the title "Stem cell characterization in disease states and stem cell-based therapies" with authorization number AP21-019, first approved on April 09, 2021. All procedures were carried out in accordance with the Kanazawa University Animal Experimentation Regulations. Throughout the experimental period, the health status of the mice was monitored by observing their activity levels, general behavior, and hair coat conditions. Other than surgical

intervention, no humane endpoints were set, as the protocol posed no risk of distress.

Consent for publication

Not applicable.

Artificial intelligence (AI)

The authors declare that they have not used Al-generated work in this manuscript.

Competing interests

The authors declare no competing interests.

Author details

¹Department of Gastroenterology, Kanazawa University Hospital, Kanazawa, Japan

²Information-Based Medicine Development, Kanazawa University, Kanazawa, Japan

³Marukawa Hospital, Nyuzen, Japan

⁴National hospital organization Kanazawa medical center, Kanazawa, Japan

⁵Sakai Clinic, Nonoichi, Japan

Received: 15 April 2025 / Accepted: 23 June 2025 Published online: 06 July 2025

References

- Estes C, Razavi H, Loomba R, Younossi Z, Sanyal AJ. Modeling the epidemic of nonalcoholic fatty liver disease demonstrates an exponential increase in burden of disease. Hepatology. 2018;67(1):123–33. https://doi.org/10.1002/hep.29466/suppinfo.
- Yeh MM, Brunt EM. Pathology of nonalcoholic fatty liver disease. Am J Clin Pathol. 2007;128(5):837–47. https://doi.org/10.1309/RTPM1PY6YGBL2G2R.
- Lim JS, Mietus-Snyder M, Valente A, Schwarz JM, Lustig RH. The role of Fructose in the pathogenesis of NAFLD and the metabolic syndrome. Nat Rev Gastroenterol Hepatol. 2010;7(5):251–64. https://doi.org/10.1038/nrgastro.2010.41.
- Fu S, Watkins SM, Hotamisligil GS. The role of Endoplasmic reticulum in hepatic lipid homeostasis and stress signaling. Cell Metab. 2012;15(5):623–34. https://doi.org/10.1016/j.cmet.2012.03.007.
- Hetz C. The unfolded protein response: controlling cell fate decisions under ER stress and beyond. Nat Rev Mol Cell Biol. 2012;13(2):89–102. https://doi.or g/10.1038/nrm3270.
- Brenner C, Galluzzi L, Kepp O, Kroemer G. Decoding cell death signals in liver inflammation. J Hepatol. 2013;59(3):583–94. https://doi.org/10.1016/j.jhep.20 13.03.033
- Li TT, Wang ZR, Yao WQ, Linghu EQ, Wang FS, Shi L. Stem cell therapies for chronic liver diseases: progress and challenges. Stem Cells Transl Med. 2022;11(9):900–11. https://doi.org/10.1093/stcltm/szac053.
- Seki A, Sakai Y, Komura T, Nasti A, Yoshida K, Higashimoto M, et al. Adipose tissue-derived stem cells as a regenerative therapy for a mouse steatohepatitis-induced cirrhosis model. Hepatology. 2013;58(3):1133–42. https://doi.org/ 10.1002/hep.26470.
- Yamato M, Sakai Y, Mochida H, Kawaguchi K, Takamura M, Usui S, et al. Adipose tissue-derived stem cells prevent fibrosis in murine steatohepatitis by suppressing IL-17-mediated inflammation. J Gastroenterol Hepatol. 2019;34(5):878–85. https://doi.org/10.1111/jgh.14647.
- Ishida K, Seki A, Kawaguchi K, Nasti A, Yamato M, Inui H, et al. Restorative effect of adipose tissue-derived stem cells on impaired hepatocytes through Notch signaling in non-alcoholic steatohepatitis mice. Stem Cell Res. 2021;54:102425. https://doi.org/10.1016/j.scr.2021.102425.
- Kitani H, Sakuma C, Takenouchi T, Sato M, Yoshioka M. Establishment of c-myc-immortalized Kupffer cell line from a C57BL/6 mouse strain. Results Immunol. 2014;4:68–74. https://doi.org/10.1016/j.rinim.2014.08.001.

- Miura N, Kanayama Y, Nagai W, Hasegawa T, Seko Y, Kaji T, et al. Characterization of an immortalized hepatic stellate cell line established from metallothionein-null mice. J Toxicol Sci. 2006;31(4):391–8. https://doi.org/10.2 131/jts.31.391.
- Malhi H, Kaufman RJ. Endoplasmic reticulum stress in liver disease. J Hepatol. 2011;54(4):795–809. https://doi.org/10.1016/j.jhep.2010.11.005.
- Hong F, Liu B, Wu BX, Morreall J, Roth B, Davies C, et al. CNPY2 is a key initiator of the PERK–CHOP pathway of the unfolded protein response. Nat Struct Mol Biol. 2017;24(10):834–9. https://doi.org/10.1038/nsmb.3458.
- Song S, Tan J, Miao Y, Li M, Zhang Q. Crosstalk of autophagy and apoptosis: involvement of the dual role of autophagy under ER stress. J Cell Physiol. 2017;232(11):2977–84. https://doi.org/10.1002/jcp.25785.
- Li Y, Yang P, Ye J, Xu Q, Wu J, Wang Y. Updated mechanisms of MASLD pathogenesis. Lipids Health Dis. 2024;23(1):117. https://doi.org/10.1186/s12944-02 4-02108-x
- Higashimoto M, Sakai Y, Takamura M, Usui S, Nasti A, Yoshida K, et al. Adipose tissue derived stromal stem cell therapy in murine ConA-derived hepatitis is dependent on myeloid-lineage and CD4+T-cell suppression. Eur J Immunol. 2013;43(11):2956–68. https://doi.org/10.1002/eji.201343531.
- Liu Q, Tang Q, Jing X, Zhang J, Xia Y, Yan J, et al. Mesencephalic astrocytederived neurotrophic factor protects against paracetamol-induced liver injury by inhibiting PERK-ATF4-CHOP signaling pathway. Biochem Biophys Res Commun. 2022;602:163–9. https://doi.org/10.1016/j.bbrc.2022.02.059.
- Gesteiro E, Guijarro L, Sánchez-Muniz FJ, Vidal-Carou MC, Troncoso A, Venanci L, et al. Palm oil on the edge. Nutrients. 2019;11(9):2008. https://doi.org/10.33 90/nu11092008.
- Zhang Y, Xue R, Zhang Z, Yang X, Shi H. Palmitic and Linoleic acids induce ER stress and apoptosis in hepatoma cells. Lipids Health Dis. 2012;11:1. https://doi.org/10.1186/1476-511X-11-1.
- Medrano M, Lemus-Conejo A, Lopez S, Millan-Linares MC, Rosillo MA, Muñiz M, et al. CD4+and CD8+T-cell responses in bone marrow to fatty acids in high-fat diets. J Nutr Biochem. 2022;107:109057. https://doi.org/10.1016/j.jnu tbio.2022.109057.
- Tan Z, Qian X, Jiang R, Liu Q, Wang Y, Chen C, et al. IL-17A plays a crucial role in the pathogenesis of liver fibrosis by activating hepatic stellate cells. J Immunol. 2013;191(4):1835–44. https://doi.org/10.4049/jimmunol.1203013.
- Fang C, Weng T, Hu S, Yuan Z, Xiong H, Huang B, et al. IFN-γ-induced ER stress impairs autophagy and triggers apoptosis in lung cancer cells. Oncoimmunology. 2021;10(1):1962591. https://doi.org/10.1080/2162402X.2021.1962591.
- Liu X, Chen Y, Wang H, Wei Y, Yuan Y, Zhou Q, et al. Microglia-derived IL-1β promoted neuronal apoptosis through ER stress-mediated signaling pathway PERK/eIF2α/ATF4/CHOP upon arsenic exposure. J Hazard Mater. 2021;417:125997. https://doi.org/10.1016/j.jhazmat.2021.125997.
- Dangi A, Huang C, Tandon A, Stolz D, Wu T, Gandhi CR. Endotoxin-stimulated rat hepatic stellate cells induce autophagy in hepatocytes as a survival mechanism. J Cell Physiol. 2016;231(1):94–104. https://doi.org/10.1002/jcp.25 055
- 26. Yang J, Xu C, Wu M, Wu Y, Jia X, Zhou C, et al. MicroRNA-124 inhibits hepatic stellate cells inflammatory cytokines secretion by targeting IQGAP1 through NF-kB pathway. Int Immunopharmacol. 2021;95:107520. https://doi.org/10.1016/j.intimp.2021.107520.
- Verstockt B, Ferrante M, Vermeire S, Van Assche G. New treatment options for inflammatory bowel diseases. J Gastroenterol. 2018;53(5):585–90. https://doi. org/10.1007/s00535-018-1449-z.
- Murata M, Teshima T. Treatment of Steroid-Refractory acute Graft-Versus-Host disease using commercial mesenchymal stem cell products. Front Immunol. 2021;12:724380. https://doi.org/10.3389/fimmu.2021.724380.
- Harley ITW, Stankiewicz TE, Giles DA, Softic S, Flick LM, Cappelletti M, et al. IL-17 signaling accelerates the progression of nonalcoholic fatty liver disease in mice. Hepatology. 2014;59(5):1830–9. https://doi.org/10.1002/hep.26746.

Publisher's note

Springer Nature remains neutral with regard to jurisdictional claims in published maps and institutional affiliations.